The Two-Dimensional Disordered Boson Hubbard Model: Evidence for a Direct Mott Insulator-to-Superfluid Transition and Localization in the Bose Glass Phase

Jens Kisker

Institut für Theoretische Physik, Universität zu Köln, D-50937 Köln, Germany

Heiko Rieger

HLRZ c/o Forschungszentrum Jülich, D-52425 Jülich, Germany
(November 28, 2001)

We investigate the Bose glass phase and the insulator-to-superfluid transition in the two-dimensional disordered boson Hubbard model in the Villain representation via Monte Carlo simulations. In the Bose glass phase the probability distribution of the local susceptibility is found to have a $1/\chi^2$ tail and the imaginary time Green's function decays algebraically $C(\tau) \sim \tau^{-1}$, giving rise to a divergent global susceptibility. By considering the participation ratio it is shown that the excitations in the Bose glass phase are fully localized and a scaling law is established. For commensurate boson densities we find a *direct* Mott insulator to superfluid transition without an intervening Bose glass phase for weak disorder. For this transition we obtain the critical exponents $z = 1, \nu = 0.7 \pm 0.1$ and $\eta = 0.1 \pm 0.1$, which agree with those for the classical three-dimensional XY model without disorder. This indicates that disorder is irrelevant at the tip of the Mott-lobes and that here the inequality $\nu \geq 2/d$ is violated.

PACS numbers: 67.40.-w, 74.70.Mq, 74.20.Mn

I. INTRODUCTION

The localization transition in disordered systems of interacting bosons has attracted a lot of interest in recent years. The observation is that there is a direct superconductor to insulator transition at zero temperature, which can be tuned by varying a suitable control parameter like the disorder strength or an applied magnetic field. The paradigmatic two-dimensional realizations of such systems are amorphous superconducting films[1], where the Cooper pairs are considered as bosons, and [4]He adsorbed in porous media[2]. On the theoretical side, these systems are described most simply by a boson Hubbard model, and a large amount of effort has been put forth to study the various aspects of this transition. This includes mean-field calculations[3], real space renormalization group studies[4], strong coupling expansions[5] and quantum Monte Carlo investigations in one-[6] and two dimensions[7–9].

Of particular interest are the properties of the so called Bose glass phase which is supposed to emerge for strong disorder, and which is characterized by being insulating but compressible and gapless[3]. The latter property leads to a diverging superfluid susceptibility throughout the Bose glass phase, which is reminiscent of the quantum Griffiths phase in random transverse Ising systems[10–14]. It is one of the main goals of this work to investigate the Bose glass phase and to characterize the Griffiths singularities by means of Monte Carlo simulations of the 2D Bose Hubbard model. The other major point of interest is the insulator to superfluid transition for weak disorder and commensurate boson densities, since there is an ongoing debate whether this transition occurs from the Mott insulating (MI)- or the Bose glass (BG) phase[3,4,8]. In this paper we present numerical evidence for a *direct* Mott insulator to superfluid transition that falls in the universality class of the pure classical XY-model in three dimensions. A short account of our results has been given recently[15].

The paper is organized as follows: In Sec. II the 2D Bose Hubbard model is introduced and it is briefly stated, how one arrives via a set of transformations at a 3D classical model, which is used subsequently in the simulations. In Sec. III we introduce the quantities of interest and summarize the scaling theory of Ref.[3] which is needed for a finite size scaling analysis of the data. In Sec. IV the Monte Carlo algorithm is presented. In Sec. V we examine the Bose glass phase for strong disorder and in Sec. VI we consider the case of weak disorder and address the question of a direct MI-SF transition.

II. THE MODEL

We consider the boson Hubbard model with disorder on a square lattice in $d = 2$ dimensions. The Hamiltonian is given by

$$H_{BH} = H_0 + H_1 \tag{1}$$

$$H_0 = -t \sum_{\langle i,j \rangle} (\hat{\Phi}_i^\dagger \hat{\Phi}_j + \hat{\Phi}_i \hat{\Phi}_j^\dagger) \tag{2}$$

$$H_1 = \frac{U}{2} \sum_i \hat{n}_i^2 - \sum_i (\mu + v_i) \hat{n}_i , \tag{3}$$

where $\hat{\Phi}_i$ ($\hat{\Phi}_i^\dagger$) is the boson annihilation (creation) operator at site i and $\hat{n}_i = \hat{\Phi}_i^\dagger \hat{\Phi}_i$ is the usual number operator.

The hopping matrix is t for nearest neighbors and zero otherwise. The bosons interact via an on-site repulsion U, μ is the chemical potential and v_i represents the random on-site potential varying uniformly in space between $-\Delta$ and Δ.

As a simplification we take the "phase-only" approximation[16], where amplitude fluctuations in (1) are integrated out. One assumes that the complex field Φ has the simple form $\Phi_i = |\Phi_0|e^{i\hat{\phi}_i}$, where $\hat{\phi}_i$ is the phase operator conjugate to the number operator $\hat{n}_i$ with commutation relation $[\phi_i, n_j] = i\delta_{ij}$. This yields the quantum-phase-Hamiltonian

$$H_{QPH} = H_0 + H_1 \qquad (4)$$

$$H_0 = -t\sum_{\langle i,j \rangle} \cos(\hat{\phi}_i - \hat{\phi}_j) \qquad (5)$$

$$H_1 = \frac{U}{2}\sum_i \hat{n}_i^2 - \sum_i (\mu + v_i)\hat{n}_i , \qquad (6)$$

where $\hat{n}_i$ now measures the deviation from a mean density.

A. Duality transformation

Through a sequence of transformations the 2D quantum mechanical Hamiltonian (4) can be mapped onto a classical model of divergence-free integer link variables in $(2+1)$ dimensions which is suitable for Monte Carlo simulations[7].

The transformation uses the standard Suzuki-Trotter[17] formula where the inverse temperature β is divided into L_τ time slices of width $\Delta\tau = \beta/L_\tau$ yielding a path integral representation of Hamiltonian (4). Taking the Villain approximation[18], which replaces the exponentiated cosine term in the partition function by a sum of periodic gaussians, and after a further Poisson summation, one can show that the ground state energy density of the quantum model (4) is equal to the free energy density of a purely classical model

$$f = \lim_{T\to 0}\frac{T}{L^2}\ln\operatorname{Tr} e^{-\beta H_{QPH}} = -\frac{1}{L^2 L_\tau \Delta\tau}\ln\operatorname{Tr} e^{-H_{\text{class}}/K} ,$$
$$(7)$$

where the classical Hamiltonian H_{class} is given by

$$H_{\text{class}} = \sum_{(i,\tau')}^{\nabla\cdot\mathbf{J}=0}\left(\frac{1}{2}\mathbf{J}_{i,\tau'}^2 - (\mu + v_i)J_{i,\tau'}^\tau\right) . \qquad (8)$$

and the parameter K acts as an effective temperature of the model and is used to tune through the phase transition. K corresponds to t/U in the quantum phase model

(4) and thus by changing K one moves horizontally, i.e. parallel to the t/U axis in the phase diagram of Hamiltonian (4). The $\mathbf{J}'s = (J^x, J^y, J^\tau)$ are three-component vectors consisting of integer variables on the links of the original lattice running from $-\infty$ to ∞. The τ-component J^τ corresponds to the particle number. Note that the summation in (8) is just over *divergence-free* configurations of the link variables. Strictly speaking, one has to take the limit $L_\tau \to \infty$ for the equality in eq. (7) to be valid. In the simulations however, we have to keep L_τ finite, which means that we are working at a temperature $T \sim 1/L_\tau$ for the original quantum phase model (4).

The action (8) describes an ensemble of string like objects in a random potential, and considering the divergence-free condition, these objects can be interpreted as flux-lines in a high-T_C superconductor. This observation is not surprising, since one has the general correspondence between 2D bosons at zero temperature and flux-lines in 3D high-T_C superconductors[19−21].

B. Phase diagram

The phase diagram of the classical Hamiltonian (8) in the thermodynamic limit ($L \to \infty$, $L_\tau \to \infty$), which corresponds to the $T = 0$ phase diagram of the quantum model (4) can be obtained qualitatively by simple perturbative arguments[3].

For the case without disorder ($v_i = 0$) one obtains two phases: a Mott insulating and a superconducting phase. In the μ vs. K plane the Mott insulating phase has a lobe like shape which can be understood by first considering the atomic limit $K = 0$ and then allow for small hopping in the quantum phase model (4), i.e. finite effective temperature for the classical model (8). At zero effective temperature, every site is occupied by an integer number $n = J^\tau$ of bosons which minimizes the on site energy $\epsilon(n) = -\mu n + \frac{1}{2}n^2$. Thus in the interval $n < \mu + \frac{1}{2} < n+1$ the occupation number is fixed to n at every site causing the compressibility $\kappa = \partial n/\partial\mu$ to vanish. Furthermore there is a gap in the single particle spectrum making the Mott phase indeed an insulator.

For increasing hopping amplitude t/U the bosons in the original quantum phase model (4) can gain kinetic energy by hopping on the lattice and thus the gap decreases with increasing t. When the gap vanishes, the bosons are free to hop on the lattice thus producing superfluidity. Equivalently in the classical model (8) an increase in effective temperature K causes a distortion of the initially straight world lines allowing them to move around freely above some critical value for K giving the Mott phase a lobe like shape. As Hamiltonian (8) is periodic in μ with period 1, the lobes are repeated on the μ axis.

In the presence of disorder a new, insulating Bose glass phase is supposed to emerge[3] in addition to the Mott

insulating and the superfluid phase. As the disorder strength Δ increases, the Mott lobes shrink since there will always be sites where the energy necessary to add a particle or hole is reduced due to the disorder and these sites therefore favour the addition of particles or holes. Thus the compressibility ceases to vanish and the trace of the Mott insulator disappears. Fisher *et al.* now argue that the extra bosons will not immediately produce superfluidity but will still be localized due to the disorder. Thus the new phase is characterized by a non-vanishing compressibility, no energy gap and zero conductivity. Only for larger hopping amplitudes the bosons will become delocalized resulting in a superfluid phase.

The phase diagram for weak disorder suggested by our simulations is depicted in Fig. 1. Note that contrary to Ref.[3] we find a *direct* MI-SF transition for integer values of the chemical potential (see Sec. VI) and therefore there is no intervening BG phase at the tip of the lobe.
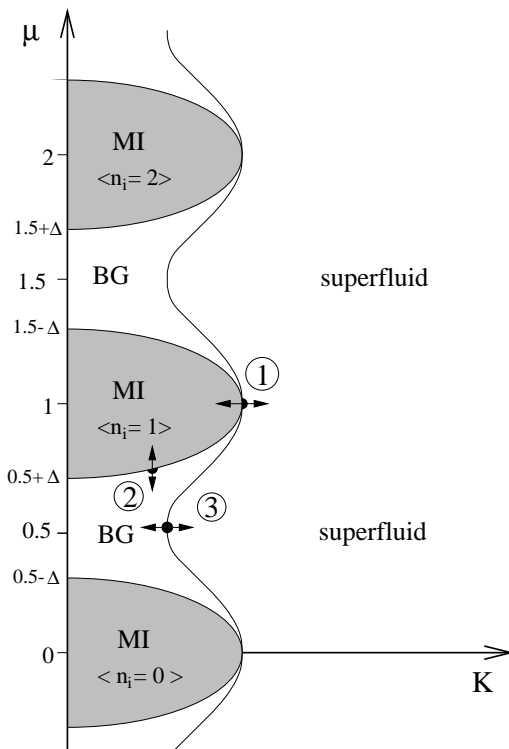

FIG. 1. The $L_\tau = \infty$ phase diagram of the classical model (8) for weak disorder suggested by our results presented in this paper. The Mott lobes are centered around integer values of the chemical potential. For integer values of μ we find a *direct* MI-SF transition at a multicritical point, therefore there is no intervening BG phase at the tip of lobe. Since the Hamiltonian (8) is periodic in the chemical potential with period one, the Mott lobes are repeated in the y-direction. The dots denote the phase transitions we examine in the simulations and are labeled for later reference. The arrows indicate whether μ or K were used to tune through the different transitions.

For disorder strengths $\Delta \geq U/2$ one obtains the phase diagram shown in Fig. 2. The Mott lobes have totally

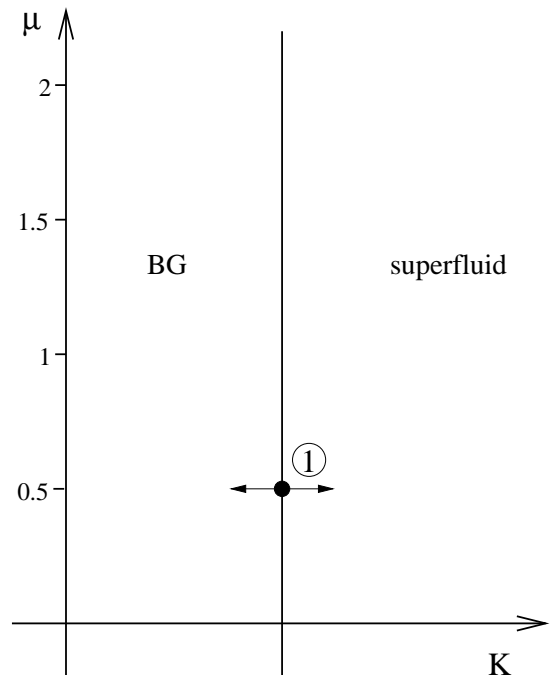disappeared and only the BG- and the superfluid phase remain.

FIG. 2. The zero temperature phase diagram of the classical model (8) for disorder strengths $\Delta \geq 1/2$. The Mott lobes have disappeared and only the BG- and the SF-phase remain. The dot denotes the BG-SF transition studied in Sec. V and is identical to point #3 in Fig. 1.

Furthermore Fisher *et al.* argue that due to the non-vanishing density of states at zero energy the imaginary time Green's function $C(\tau)$ decays algebraically in the BG phase. This leads to a divergent superfluid susceptibility $\chi = \int C(\tau) \, d\tau$ in the BG phase, which thus resembles the quantum Griffiths phase found in other disordered systems[10−14]. We investigate this scenario in Sec. V.

III. SCALING THEORY AND FINITE-SIZE SCALING

For completeness we give a brief summary of the $T = 0$ scaling theory developed in Ref.[3]. Furthermore we introduce the quantities of interest and show how they can be expressed in terms of the link variables of the classical model (8). Since in the simulations we are working with finite systems, it is also shown how to obtain results via finite-size scaling.

A. Stiffness

From the anisotropy of the classical model (8) it can be seen, that near a continuous phase transition there

are two diverging correlation "lengths" ξ and ξ_τ. This is due to the fact that we are considering a $T = 0$ quantum phase transition where static and dynamic properties of a system are linked. ξ is the correlation length in the spatial directions, whereas ξ_τ denotes a diverging time scale in the imaginary time direction. As usual we introduce the critical exponent ν by $\xi \sim \delta^{-\nu}$. Generally ξ_τ will diverge with a different exponent so we define the dynamical critical exponent z by $\xi_\tau \sim \xi^z$. The control parameter δ measures the normalized distance from the critical point, which is $\delta = (K - K_C)/K_C$ or $\delta = (\mu - \mu_C)/\mu_C$ in the simulations.

An important quantity in the further analysis is the zero frequency stiffness $\rho(0)$, which is proportional to the order parameter, i.e. the condensate. Thus by calculating the stiffness we are able to locate the critical point of a phase transition from an insulating to a superconducting phase. The stiffness measures the change of the free energy under imposing a twist θ in the phase of the order parameter and is defined by

$$\frac{\delta f_s}{\hbar} = \frac{1}{2}\rho(\nabla\theta)^2 \ , \tag{9}$$

where f_s denotes the singular part of the free energy. Via hyperscaling the scaling form

$$\rho \sim \xi^{-(d+z-2)} \tag{10}$$

can be derived[3].

To calculate the stiffness in the simulations we have to express ρ in terms of the link variables of the classical model (8). By considering the effect of an external vector potential one obtains[7]

$$\rho(0) = \frac{1}{L_\tau}[\langle n_x^2 \rangle]_{\text{av}} \ , \tag{11}$$

where n_x defines the winding number

$$n_x = \frac{1}{L} \sum_{(i,\tau)} J_{(i,\tau)}^x \ , \tag{12}$$

and $[\ldots]_{\text{av}}$ denotes a disorder average. Since at the critical point the diverging correlation lengths are much larger than the system size we need to obtain a finite-size scaling form of the stiffness to analyse our data. Because there are two diverging correlation lengths, all quantities will depend on the ratios L/ξ and L_τ/ξ_τ. By considering this and eq. (10) we get

$$\rho(0) = \xi^{-(d+z+2)} P(L/\xi, L_\tau/\xi_\tau) \ , \tag{13}$$

which can be expressed as

$$\rho(0) = \frac{1}{L^{d+z-2}} \tilde{\rho}(L^{1/\nu}\delta, L_\tau/L^z) \ , \tag{14}$$

where P and $\tilde{\rho}$ are scaling functions. Thus we see that by keeping the *aspect ratio* $a = L_\tau/L^z$ constant, the scaling

function $\tilde{\rho}$ just depends on one argument. This enables us to locate the critical point, since at criticality $\delta = 0$ and $L^{d+z-2}\rho(0)$ then is independent of L, which means that a plot of $L^{d+z-2}\rho(0)$ vs. K for different system sizes with constant aspect ratio yields an intersection point at the critical point.

B. Compressibility

In a similar way as for the stiffness, a scaling expression for the compressibilty

$$\kappa = \frac{\partial n}{\partial \mu} \tag{15}$$

can be derived. By imposing a twist in the phase of the order parameter in the imaginary time direction instead of the space directions, one obtains the scaling form

$$\kappa \sim \xi^{-(d-z)} \ , \tag{16}$$

and the corresponding finite-size scaling form is

$$\kappa(0) = \frac{1}{L^{d-z}}\tilde{\kappa}\left(L^{1/\nu}\delta, \frac{L_\tau}{L^z}\right) \ . \tag{17}$$

Since by definition κ measures the fluctuations in the particle number, which is given by the J_i^τ's in the classical model (8), κ can be expressed in terms of the link variables as[7]

$$\kappa(0) = \frac{1}{L^d L_\tau}[\langle N_b^2 \rangle - \langle N_b \rangle^2]_{\text{av}} \ , \tag{18}$$

where $N_b = \sum_{i,\tau'} J_{i,\tau'}^\tau$.

C. Correlation functions

In addition to ν and z a third critical exponent η can be introduced by considering the correlation function $C(\mathbf{r}, \mathbf{r}', \tau, \tau')$ for creating a boson at point $(\mathbf{r}, \tau)$ and destructing it at $(\mathbf{r}', \tau')$. In the quantum phase model (4) this correlation function is given by

$$C(\mathbf{r}, \mathbf{r}', \tau, \tau') = [\langle e^{i[\hat{\phi}_{\mathbf{r}'}(\tau') - \hat{\phi}_{\mathbf{r}}(\tau)]} \rangle]_{\text{av}} \ , \tag{19}$$

and due to the disorder average $C(\mathbf{r}, \mathbf{r}', \tau, \tau')$ will be translationally invariant, i.e. $C(\mathbf{r}, \mathbf{r}', \tau, \tau') = C(\mathbf{r} - \mathbf{r}', \tau - \tau')$. We will only be interested in the equal time correlation function $C_x(r) = C(r, 0)$ and the time dependent correlation function $C_+(\tau) = C(0, \tau)$, which is essentially a Green's function.

The spatial correlation function $C_x(r)$ can be expressed in terms of the link variables as[7]

$$C_x(r) = \left[\left\langle \prod_{\mathbf{r}\in\text{path}} \exp\left\{-\frac{1}{K}\left(J_{(\mathbf{r},\tau)}^x + \frac{1}{2}\right)\right\}\right\rangle\right]_{\text{av}} \tag{20}$$

4

where "path" is a straight line connecting two points a distance r apart in the x-direction with τ fixed. Since the classical action (8) is invariant under the transformation $J_x \to -J_x$ it follows that $C_x(r) = C_x(-r)$.

For the time dependent correlation function a similar expression can be derived. However, due to the lack of general particle-hole symmetry of Hamiltonian (4), the correlation functions for particles $C_+(\tau)$ and holes $C_-(\tau)$ will generally be different, except for the case when $\mu = n/2$ with n integer, since then statistical particle-hole symmetry is restored. For the single site time dependent correlation function one obtains

$$C_+^i(\tau) = \left\langle \prod_{\tau' \in \text{path}} \exp\left\{ -\frac{1}{K}\left(\frac{1}{2} + J_{(i,\tau')}^\tau - \mu_i \right) \right\} \right\rangle , \tag{21}$$

where "path" is a straight line connecting two points with fixed $\mathbf{r}$ a distance τ apart in the (imaginary) time direction. The site and disorder averaged correlation function $C_+(\tau)$ is then defined as

$$C_+(\tau) = [C_+^i(\tau)]_{\text{av}}. \tag{22}$$

A similar expression can be derived for $C_-(\tau)$. The single site function $C_+^i(\tau)$ corresponds to the local imaginary time Green's function $\langle \Phi_i(\tau)\Phi_i^+(0)\rangle$ in the original Bose Hubbard model (1).

According to Ref.[3] a scaling form for $C(\mathbf{r}, \tau)$ can be derived under the assumption that the long-distance and long-time behaviour depends on the ratios r/ξ and τ/ξ_τ. This yields

$$C(\mathbf{r}, \tau) = r^{-(d+z-2+\eta)} f(r/\xi, \tau/\xi^z) , \tag{23}$$

with a scaling function f and critical exponent η. It follows that at criticality

$$C_x(r) \sim r^{-y_x} \quad \text{and} \quad C_+(\tau) \sim \tau^{-y_\tau} , \tag{24}$$

where y_x and y_τ are given by

$$y_x = d - 2 + z + \eta \tag{25}$$

and

$$y_\tau = (d - 2 + z + \eta)/z . \tag{26}$$

Thus if one is able to determine y_x and y_τ in the simulations, z and η can be calculated from

$$z = y_x/y_\tau \tag{27}$$

and

$$\eta = y_x - d + 2 - y_x/y_\tau . \tag{28}$$

IV. MONTE CARLO ALGORITHM

The Monte Carlo algorithm has to account for the zero divergence condition of the link variables. Following Ref.[7] we choose our update procedure to consist of local and global moves. In a local move four link variables on an elementary plaquette are changed simultaneously. Two of the link variables are incremented and the two other are decremented by one, thus fulfilling the zero divergence condition. The inverse of such a local move is also used, i.e. a configuration where the pluses and minuses are exchanged. Global moves consist of changing a whole line of link variables extending all through the system by ± 1 and are performed in all three directions x, y and τ. We apply periodic boundary conditions, so the zero divergence condition is also fulfilled. A global move in the τ direction amounts to injecting or destructing a boson, since the τ component J_i^τ of the link variables measures the particle number. Thus when one explicitly wishes to keep the number of particles constant as in Sec. V B, global moves in the τ direction have to be either excluded or they have to be performed pairwise, i.e. one creates and destructs a boson at two different sites simultaneously.

For a given configuration of the link variables we then perform a local or global move and calculate the energy difference ΔE between these two states. We use the heat-bath algorithm, where the new configuration is accepted with probability

$$w(\Delta E) = \frac{1}{1 + \exp(\Delta E/K)} . \tag{29}$$

Time is measured in Monte Carlo steps (MCS), where one step corresponds to a sweep of local and global moves through the whole lattice.

Since we are interested in equilibrium properties of the system equilibration is an important issue. In order to have a criterion for equilibration we proceed as in Ref.[7] where a method used for spin glasses[22] has been adapted. We consider two replicas α and β of a system with the same realization of disorder and calculate the "Hamming"-distance, which is defined as

$$h_{\alpha,\beta}^\nu(t_0) = \left[\sum_{t=t_0}^{2t_0} \sum_{(i,\tau)} \left[J_{(i,\tau)}^{v,\alpha}(t) - J_{(i,\tau)}^{v,\beta}(t) \right]^2 \right]_{\text{av}} , \tag{30}$$

where t_0 is a suitably chosen equilibration time and $\nu = x, y, \tau$. We also calculate the "Hamming"-distance for one replica given by

$$h_\alpha^\nu(t_0) = \left[\sum_{t=t_0}^{2t_0} \sum_{(i,\tau)} \left[J_{(i,\tau)}^{\nu,\alpha}(t + t_0) - J_{(i,\tau)}^{\nu,\alpha}(t_0) \right]^2 \right]_{\text{av}} . \tag{31}$$

When t_0 is chosen sufficiently large, the system is equilibrated and one should have $h_{\alpha,\beta}^\nu(t_0) = h_\alpha^\nu(t_0)$. Thus

by choosing a sequence of increasing values of $t_0 = 10, 30, 100, 300, \ldots$ one can give an estimate for the equilibration time from the coincidence of two values.

The equilibration time increases drastically with system size. We found that for smaller systems (e.g. 6x6x9) ≈ 5000 MCS were sufficient, whereas the larger lattice sizes (10x10x25) took about 10^5 MCS. The equilibration time mainly depends on the system size L in the spatial directions, since the disorder, which only enters the transition probability of global moves in the τ direction, enhances the acceptance rate for this type of moves. This made it possible to study systems with large L_τ such as 8x8x200, which became necessary to avoid finite-size effects when calculating the probability distribution of the local susceptibility in Sec. V.

One also has to consider the disorder average $[\ldots]_{\mathrm{av}}$. The number of samples necessary to get decent statistics strongly depends on the quantity of interest. For the stiffness (see Section VI) some 100 samples were sufficient while the compressibility has much larger sample to sample fluctuations and made it necessary to average over up to 3000 samples. This number of samples was also needed for the probability distribution of the susceptibility.

The simulations were performed on two massively parallel computers, a Parsytech GCel Transputer Cluster with 1024 T-805 transputer nodes and a Paragon X/PS 10 with 140 i860 processors.

V. BOSE GLASS PHASE

In this section we systematically investigate the Bose glass phase and work out the similarities to the quantum Griffiths phase observed in random transverse Ising systems. We choose the "strongest" possible disorder $\Delta = 0.5$, so that the Mott lobes totally disappear and only the Bose glass- and the superfluid phase remain. Furthermore throughout this section we assume $\mu = 1/2$, which corresponds to half filling.

A. Green's functions and the local susceptibility

In Ref.[3] it is argued that due to a non-vanishing density of states at zero energy the disorder averaged imaginary time Green's function $C_+(\tau)$ decays algebraically

$$C_+(\tau) \sim \tau^{-1} \qquad (32)$$

throughout the Bose glass phase. As a consequence, the superfluid susceptibility $\chi = \int C(\tau)d\tau$ is supposed to diverge in the BG phase and not only a criticality. This behaviour is similar to the quantum Griffiths phase observed in other models, such as the random transverse Ising chain[12] or the Ising spin glass in a transverse magnetic field[13,14], where various susceptibilities also diverge within part of the disordered phase.

To verify the above scenario we calculate the imaginary time Green's function and the probability distribution of the local susceptibility in the simulations.
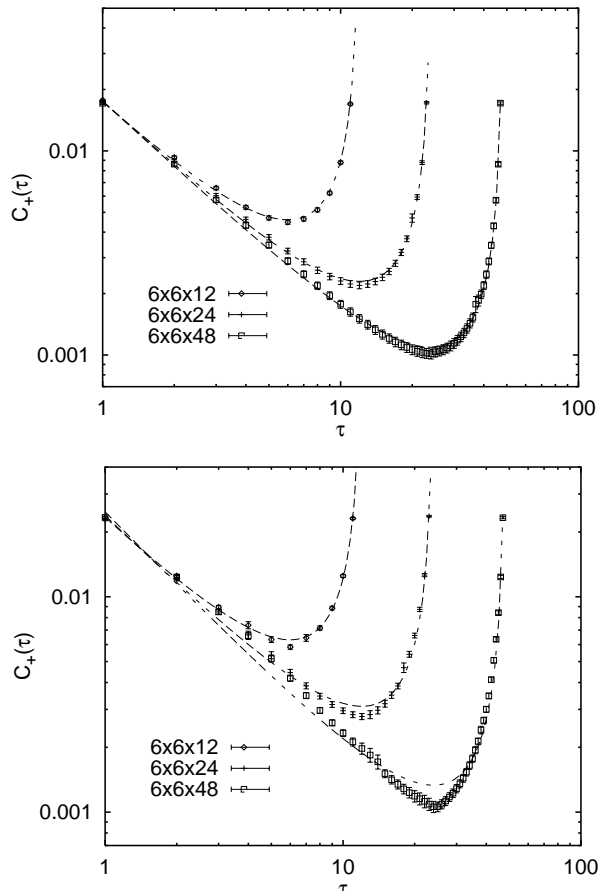

FIG. 3. The imaginary time Green's function $C_+(\tau)$ for $K = 0.17$ (top) and $K = 0.22$ (bottom) in the Bose glass phase for different system sizes. The dashed lines are fits to $C_+(\tau) = a(\tau^{y_\tau} + (L_\tau - \tau)^{y_\tau})$. The exponent y_τ is independent of the system size and independent of K. We get $y_\tau = -1.08 \pm 0.03$.

For the chosen disorder strength $\Delta = 0.5$, the phase diagram of Hamiltonian (4) consists of a Bose glass phase for small hopping amplitudes t (i.e. small values of the coupling K in the classical model (8)) and a superfluid phase for large values of t (see Fig. 2). In order to study the Bose glass phase, we have to locate the critical point for the BG-SF transition (Point #1 in Fig. 2) for the chemical potential $\mu = 0.5$ we are considering. This can be accomplished by a finite-size scaling analysis of the stiffness as pointed out in Sec. III A. We find the critical coupling $K_C(\Delta = 0.5, \mu = 0.5) = 0.247 \pm 0.003$. This phase transition was also intensively investigated in Ref.[7] in the same representation, and the value of K_C reported there perfectly agrees with the one we found.

We now investigate the BG phase for couplings $K < K_C = 0.247$. We start by calculating the Green's func-

tion $C_+(\tau)$ given by eq. (22), which is shown in Fig. 3 for couplings $K = 0.17$ and $K = 0.22$.

One observes that $C_+(\tau)$ indeed decays algebraically as

$$C_+(\tau) \sim \tau^{-1} \qquad (33)$$

within the error bars and that there is no dependence of the exponent on the system size. Similar plots can be made for other values of the coupling K in the BG phase, and one obtains the same exponent.

Relation (33) leads to a diverging superfluid susceptibility $\chi \sim \int C(\tau) d\tau$. A convenient quantity to further characterize the susceptibilty is the probability distribution of the *local*, i.e. single site susceptibility. For a diverging superfluid susceptibility a broad distribution of local susceptibilities is expected. We calculate the local susceptibility χ_i and the corresponding probability distribution $P(\chi_i)$, where χ_i is defined as

$$\chi_i = \sum_{\tau=1}^{L_\tau} C_+^i(\tau) . \qquad (34)$$

Since we expect the distribution $P(\chi_i)$ to be very broad, it is convenient to work on a logarithmic scale, i.e. we consider $P(\ln \chi_i)$ rather than $P(\chi_i)$.
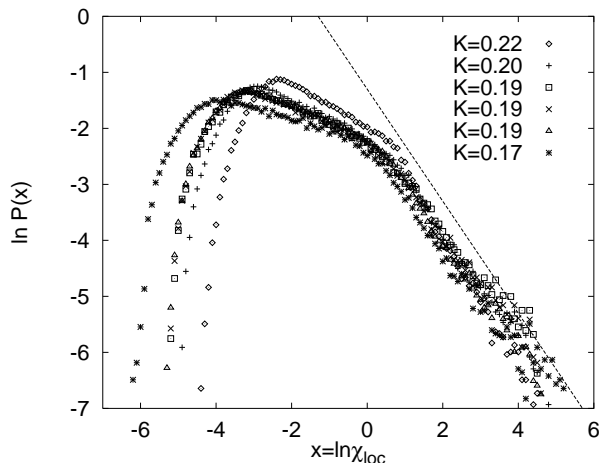

FIG. 4. The probability distribution $P(\ln \chi_{loc})$ of the local susceptibility for various values of $K < K_C = 0.247$ in the Bose glass phase ($\Delta = 0.5, \mu = 0.5$). The system size is $L = 6$ and $L_\tau = 200$. For $K = 0.19$, also data for $L = 4$ and $L = 10$ are shown, which is indistinguishable from $L = 6$. The dashed line has slope -1.

Fig. 4 shows $P(\ln \chi_i)$ for different couplings K and system sizes in the Bose glass phase. One clearly observes asymptotically ($\chi \gg 1$) a linear relation between $\ln P(\ln \chi)$ and $\ln \chi$ corresponding to an algebraic decay $P(\ln \chi) \sim \chi^{-\zeta}$ with $\zeta = 1$. Since $P(\ln \chi) = \chi P(\chi)$ this is equivalent to

$$P(\chi) \sim \chi^{-2} . \qquad (35)$$

Following the argument put forward in Ref.[13] for the corresponding quantity in the quantum Griffiths phase of

the transverse Ising spin glass one can thus introduce a dynamical exponent z: The large values of χ_i originate in local clusters containing the site i that would have a small energy gap if isolated from the rest of the sample. In the extreme case of vanishing coupling K they simply come from the sites with a local chemical potential that lends a small energy difference between single or double occupied sites $n_i = 1$ or 2, i.e. $v_i = 0$. Thus the probability for such a value of χ_i is proportional to the volume of the system $P(\chi) \sim L^d$. On the other hand, one can relate the length scale L with the inverse of the energy scale χ in the usual way introducing a dynamical exponent z via

$$P(\chi) \sim \tilde{p}(L^z/\chi) . \qquad (36)$$

With

$$\chi P(\chi) \sim L^d \chi^{-\zeta} = (L^z/\chi)^{d/z} \qquad (37)$$

we obtain

$$\ln P(\ln \chi) = -\frac{d}{z} \ln \chi + \text{const.} \qquad (38)$$

with $z = d/\zeta$. With $\zeta = 1$ it follows that $z = d = 2$ throughout the BG phase. Note that here $z = d$ in the Bose glass phase *and* at the critical point, although the two exponents have their origin in different physics: the dynamical exponent z used in eq. (38) has its origin in purely local effects, whereas the critical exponent z describes global, collective excitations at the critical point.
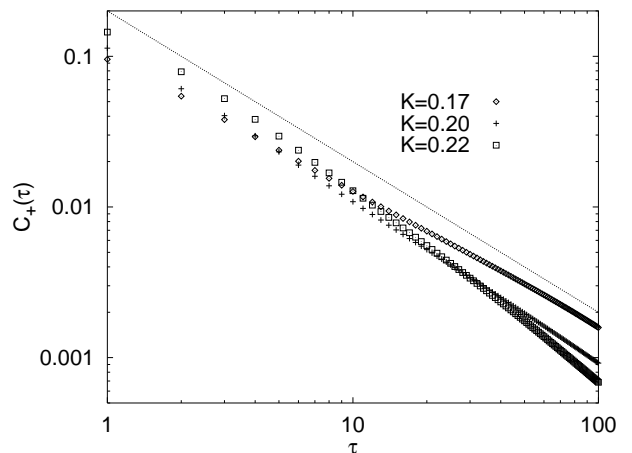

FIG. 5. $C_+(\tau)$ obtained by Laplace transformation (eq. (39)) of $P(\chi)$ for different couplings K in the BG phase. The dashed line is $\sim \tau^{-1}$. The exponent -1 is in agreement with the one calculated directly from the correlation function $C_+(\tau)$ (see Fig. 3).

If we suppose an exponential decay $C_+^i \sim \exp(-\tau/\chi_i)$, where χ_i is an effective inverse correlation length in the τ direction, we can calculate the averaged correlation function $C_+(\tau) = [C_+^i(\tau)]_{av}$ from

$$C_+(\tau) = \int_0^\infty P(\chi) \exp(-\tau/\chi) d\chi . \qquad (39)$$

Thus we have a nice consistency check for our data by recalculating $C_+(\tau)$ from $P(\chi)$. Fig. 5 shows the resulting curves for $C_+(\tau)$ for different values of $K < K_C = 0.247$. By comparison with the dotted line, one again establishes that $C_+(\tau) \sim \tau^{-1}$.

The asymptotic decay of $P(\chi) \sim \chi^{-2}$ that can be clearly seen in Fig. 4 indicates that the underlying physics is purely local. In order to see this we consider the imaginary time Green's function for $T = 0$ in the limit of zero hopping $t = 0$. Starting from the definition

$$C_+^i(\tau) = \langle n_i^0 | \Phi_i(\tau) \Phi_i^+(0) | n_i^0 \rangle \qquad (40)$$

and substituting $\Phi(\tau) = e^{\tau H} \Phi(0) e^{-\tau H}$, one obtains

$$C_+^i(\tau) \sim e^{\tau[\epsilon(n_i^0) - \epsilon(n_i^0 + 1)]} , \qquad (41)$$

where n_i^0 is the ground state occupation number at site i. From Hamiltonian (4) the energy difference for the states with n_i and $n_i + 1$ bosons at site i for $t = 0$ can be readily calculated. We obtain $\epsilon(n_i) - \epsilon(n_i + 1) = -(n_i + 1/2 - \mu - v_i)$. Since we are working at half filling $\mu = 1/2$, and $v_i \in [-1/2, 1/2]$, it follows that the on-site energy is minimized by $n_i = 0$ for $v_i < 0$ and $n_i = 1$ for $v_i > 0$. For $v_i = 0$ the states with $n_i = 0$ and $n_i = 1$ are degenerate. As a result we obtain

$$C_+^i(\tau) = \begin{cases} e^{v_i \tau} & v_i < 0 \\ e^{(v_i - 1)\tau} & v_i > 0 \end{cases} . \qquad (42)$$

From the definition $\chi_i(\omega = 0) = \int_0^\infty d\tau C_+^i(\tau)$ it then follows

$$\chi_i(\omega = 0) = \begin{cases} \frac{1}{|v_i|} & v_i < 0 \\ \frac{1}{1 - v_i} & v_i > 0 \end{cases} , \qquad (43)$$

and since $P(v)$ is uniform in the interval $[-1/2, 1/2]$, one finally obtains

$$P(\chi) \sim \frac{1}{\chi^2} . \qquad (44)$$

From this we see that the observed decay (35) of $P(\chi)$ can be explained under the assumption that the excitations in the BG phase are fully *localized* and the sites are essentially decoupled. In particular it turns out that increasing the coupling K between sites does not change the strength of the singularity in (35) significantly, implying that the dynamical exponent z does not change from $K = 0$ ($z=2$) to K_C. This is in contrast to what happens in the otherwise equivalent quantum Griffiths phase in random transverse Ising models[12,13], where an increase of the coupling between the spins leads to a continous change of the strength of the Griffiths singularities, i.e. to a continously varying dynamical exponent.

The reason for this different behaviour of the Bose glass phase in the disordered boson Hubbard model and the Griffiths phase in the random transverse Ising model is the fact that the former is related to an XY-model

whereas the latter is an Ising model. The effect of strongly coupled clusters on the dynamics (in imaginary time) is much weaker for vector spins than for Ising spins in analogy to the relaxational dynamics in classical spin models within the Griffiths phase[23].

To clarify this point and to obtain information about the localization of the excitations in the present model, we consider the participation ratio in the following section.

B. Participation ratio

In the context of localization in disordered quantum mechanical systems one usually studies a quantity called the participation ratio, which is defined with respect to one-particle excitations. Given the latter in the space representation (e.g. ψ_i) one obtains via the local probabilities $\rho_i = |\psi_i|^2$ the information about the degree of localization of this one-particle excitation by considering the ratio of moments. Since the MC algorithm we use provides us with information on the ground state exclusively (not on excitations), we devise an alternative method: we add an extra particle to the system and study how it distributes its local probabilities ρ_i among the lattice sites i. To this end we have to keep track of the local particle densities of the system with and without this extra boson - the difference is then interpreted as the probability density ρ_i of the extra boson. The degree of localization can then be read from the participation ratio

$$p_L = \left[\sum_{i=1}^N \langle \rho_i \rangle^2 \right]_{\mathrm{av}}^{-1} . \qquad (45)$$

For a fully localized state $\rho_i = \delta_{ij}$ it is $p_L = \mathcal{O}(1)$, whereas for a completely delocalized state $\rho_i = 1/N$ one has $p_L = \mathcal{O}(N)$.
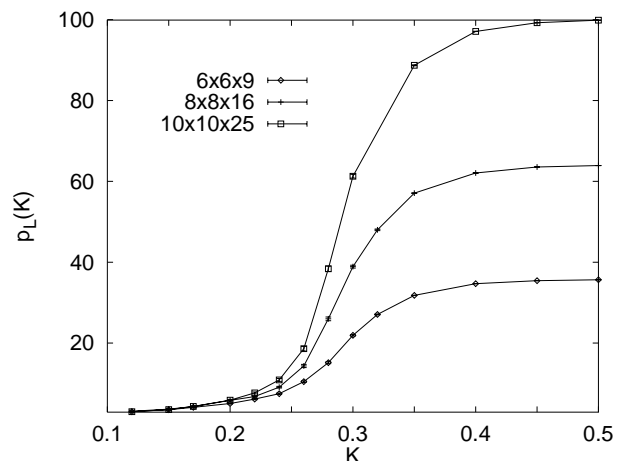

FIG. 6. The participation ratio $p_L(K)$ defined in eq. (45) as a function of K for various system sizes ($\Delta = 0.5, \mu = 0.5$). Within the Bose glass phase ($K < K_C = 0.247$) p_L approaches a constant.

To calculate p_L in the simulations we use a replica method. We consider two replicas α and β with the same realization of disorder and with fixed number of particles. Replica α is initialized with $N/2 + 1$ and replica β with $N/2$ bosons, corresponding to the case of half filling $\mu = 1/2$ considered in the preceding calculations. We then calculate the probability ρ_i of finding the excess boson at site i by

$$\rho_i = \frac{1}{L_\tau} \sum_{\tau'=1}^{L_\tau} (J_{i,\tau'}^{\tau,\alpha} - J_{i,\tau'}^{\tau,\beta}) \, . \qquad (46)$$

The restriction of working with a fixed number of particles in each replica makes it necessary to specifically consider the global moves in the τ direction in the Monte Carlo algorithm, since they amount to either injecting or destructing a boson. In a first attempt one can simply eliminate this type of move, but it turned out that it was impossible to equilibrate the systems within a reasonable amount of computer time this way. Alternatively, one can also keep the number of particles constant by injecting and destructing a particle at two different sites simultaneously. We found that by randomly choosing two sites where at one site a particle is injected and at the other a particle is destructed, the equilibration time is drastically reduced, enabling us to obtain equilibrium results.
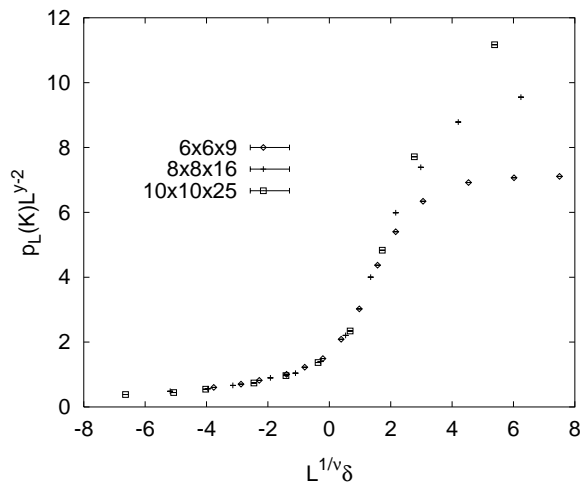

FIG. 7. Scaling Plot of the participation ratio $p_L(K)$ with $\nu = 0.9$ and $y = 1.0 \pm 0.1$.

Fig. 6 shows p_L for different system sizes with fixed aspect ratio $1/4$ and for different couplings K. One observes that the participation ratio increases with K until it eventually saturates. At saturation it is indeed as expected $p = \mathcal{O}(N)$, which tells us that in the superfluid phase the extra boson is completely delocalized. For lower couplings however, the participation ratio approaches 1 with decreasing K independent of the system size, which indicates that the extra boson is localized on a single site. We remark again that the phase transition from the Bose glass to the superfluid phase occurs at $K_C = 0.247$.

By inspection of Fig. 6 and motivated by a recent result within mean-field theory[24], one might expect that the participation ratio satisfies a scaling law. As an ansatz for a scaling relation we make

$$\frac{p_L(K)}{L^2} = L^{-y} \tilde{q}(L^{1/\nu}\delta, L_\tau/L^z) \, , \qquad (47)$$

where the scaling function $\tilde{q}$ and an additional exponent y have been introduced. $\delta = (K - K_C)/K_C$ is the distance from the critical point and ν the correlation length exponent. The values $K_C = 0.247$ and $\nu = 0.9$ can be obtained from a scaling analysis of the stiffness according to Sec. III A and the values found are in agreement with the values reported in Ref.[7]. We emphasize that we work at fixed aspect ratio $L_\tau/L^z = 1/4$, so that the scaling function $\tilde{q}$ just depends on one argument and the only variable to be determined is y. Fig. 7 shows a scaling plot of the participation ratio. The data scales nicely as long as the participation ratio is not saturated. We obtain best scaling for $y = 1.0 \pm 0.1$.
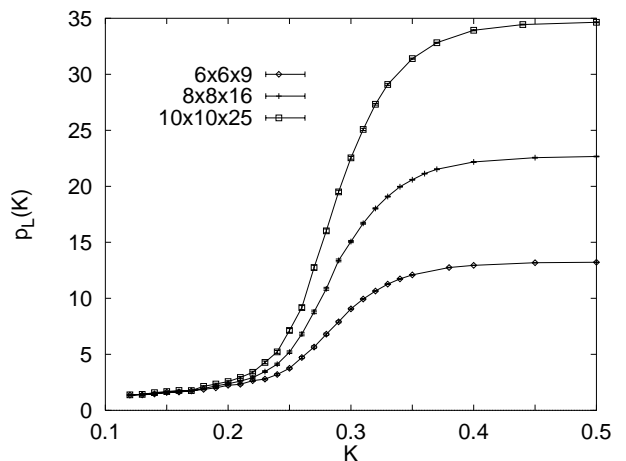

FIG. 8. The participation ratio $\tilde{p}_L(K)$ defined in eq. (48) as a function of K for various system sizes. Within the Bose glass phase ($K < K_C = 0.247$) $\tilde{p}_L$ approaches a constant.

We also considered different moments of the probability ρ_i. For instance, we calculated

$$\tilde{p}_L = \left[\left\langle \frac{(\sum_i \rho_i^2)^2}{\sum_i \rho_i^4} \right\rangle \right]_{\text{av}} , \qquad (48)$$

which is shown in Fig. 8. One observes that the curves look very similar to the ones in Fig. 6 and one obtains the same information about the localization of the excitations: for $K < K_C = 0.247$ $\tilde{p}_L$ approaches 1 independent of the system size indicating again the localization of the excitations in the BG phase, whereas for larger values of K it is $\tilde{p}_L \sim \mathcal{O}(N)$ meaning that the excitations are delocalized. We found that it is easier to calculate $\tilde{p}_L$ in the simulations than $p_L(K)$, as it turned out that the equilibration time for $\tilde{p}_L$ is much shorter than for p_L. This is the reason why we have more data points for $\tilde{p}_L$, making the curves look smoother. A scaling plot of $\tilde{p}_L$

9

according to eq. (47) is shown in Fig. 9. We find the same exponent $y = 1.0 \pm 0.1$ as for the other definition of the participation ratio in eq. (45).
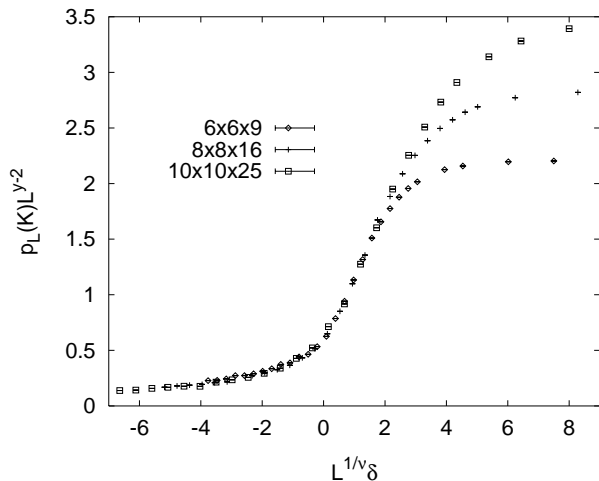

FIG. 9. Scaling Plot of the participation ratio $\tilde{p}_L(K)$ with $\nu = 0.9$ and $y = 1.0 \pm 0.1$.

VI. PHASE DIAGRAM AND PHASE TRANSITIONS FOR WEAK DISORDER

In this section we consider the model (8) for disorder strength $\Delta = 0.2$. In particular we examine the phase diagram at the tip of the lobe, i.e. at $\mu = 1$ (Point #1 in Fig. 1), where it is not clear whether there is a direct Mott insulator to superconductor phase transition or if an intervening Bose glass phase exists. Without disorder this phase transition is in the universality class of the 3D XY-model. In their scaling theory Fisher *et al.* argue that for every disorder strength $\Delta \neq 0$ the Mott lobes are surrounded by a Bose glass phase even at the tip of the lobe and consequently, the insulator-superconductor transition always occurs from the Bose glass phase. To check this prediction and to determine the critical exponents we perform a finite-size scaling analysis of the stiffness and the compressibility and also investigate the Mott insulator to Bose glass transition. Furthermore we calculate the probability distribution of the local susceptibility $P(\ln \chi)$ in the Mott insulating and the superfluid phase.

A. Finite-size scaling analysis at the tip of the lobe($\mu = 1$)

The relevant quantities of interest are the stiffness ρ and the compressibility κ, since they allow for a distinction of the different phases. We remark again that the stiffness vanishes in the Mott insulating and the Bose glass phase but is finite in the superfluid phase, whereas

the compressibility is zero in the Mott insulating phase and finite in the Bose glass and the superfluid phase.

Since for a finite-size scaling analysis according to Sec. III the aspect ratio L_τ/L^z has to be kept constant, and the dynamical exponent z is not known a priori, we first have to make a choice for z. However, by calculating the correlation functions (20) and (22) at criticality, we obtain z independent of the aspect ratio, and thus we have a consistency check for the assumed value of z.
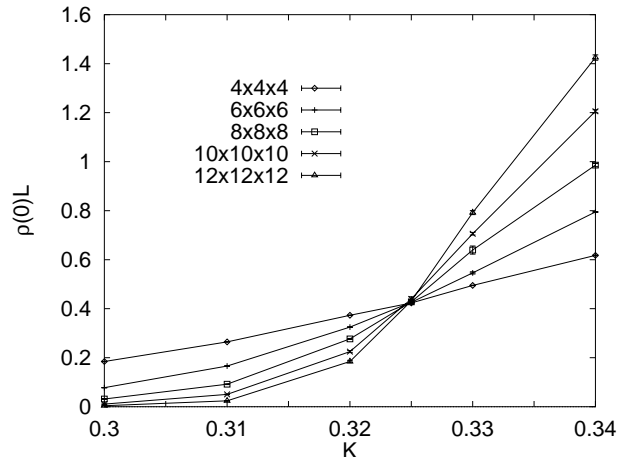

FIG. 10. The stiffness $\rho(0)L$ at the tip of the lobe ($\Delta = 0.2, \mu = 1.0$). The aspect ratio is constant for $z = 1$. The intersection point is seen to be at $K_C(\Delta = 0.2, \mu = 1) = 0.325 \pm 0.003$.

We proceed by first assuming $z = 1$ which is the value for the pure case and remark that the following calculation of the correlation functions shows that this is indeed the correct value. We calculate the stiffness ρ as given by eq. (11) and perform a finite-size scaling plot guided by eq. (14), i.e. we plot $L^{d+z-2}\rho$ vs. K for different system sizes but with constant aspect ratio $L_\tau/L^z = 1$. At the critical point $L\rho$ should be independent of L, so at criticality we expect an intersection of the different curves. Fig. 10 shows the corresponding plot. One clearly observes an intersection point at the critical coupling $K_C(\Delta = 0.2, \mu = 1) = 0.325 \pm 0.002$. For $K \leq K_C$ the stiffness scales to zero with increasing system size which indicates an insulating phase. According to Ref.[3], the Bose glass to superfluid transition always has $z = 2$, which suggests that the transition from the insulating side is from the Mott insulator rather than the Bose glass phase. The critical point is marked as point # 1 in Fig. 1.

The critical exponent ν can be obtained from a scaling plot of the stiffness. In Fig. 11 we plot $L^{d+z-2}\rho$ vs. $L^{1/\nu}\delta$ and adjust ν as to achieve best data collapse where $\delta = (K - K_C)/K_C$ with $K_C = 0.325$. One observes that the data scale nicely and we obtain $\nu = 0.7 \pm 0.1$.
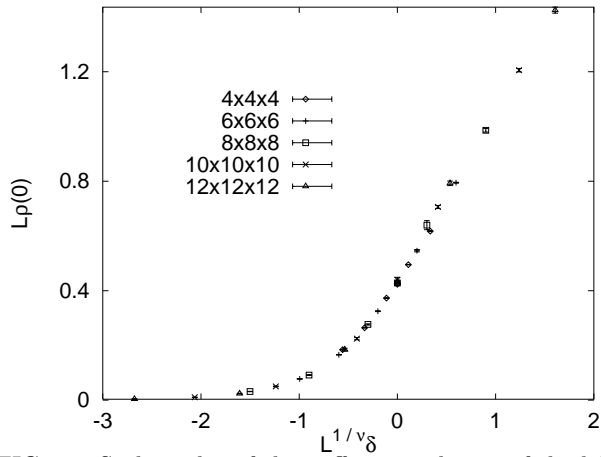
10

FIG. 11. Scaling plot of the stiffness at the tip of the lobe ($\Delta = 0.2, \mu = 1$) with $K_C = 0.325$ and $\nu = 0.7 \pm 0.1$.

We proceed by calculating the compressibility κ according to eq. (18). Fig. 12 shows a finite-size scaling plot of κ with $z = 1$. One again observes an intersection point close to $K = 0.325$, even though the intersection point is not as good as the one for the stiffness. This is due to fact that the compressibility has much larger sample to sample fluctuations than the stiffness and so it is more difficult to obtain good statistics. Note that the number of samples for the compressibility already is 2500, whereas for the stiffness 250 samples were sufficient. The large fluctuations also limited the range of system sizes we were able to simulate for the compressibility, so we only have data up to systems of size $8 \times 8 \times 8$. For couplings $K < K_C = 0.325$ we see that $L\kappa$ decreases with increasing system size, which indicates that in the thermodynamic limit $\kappa = 0$.
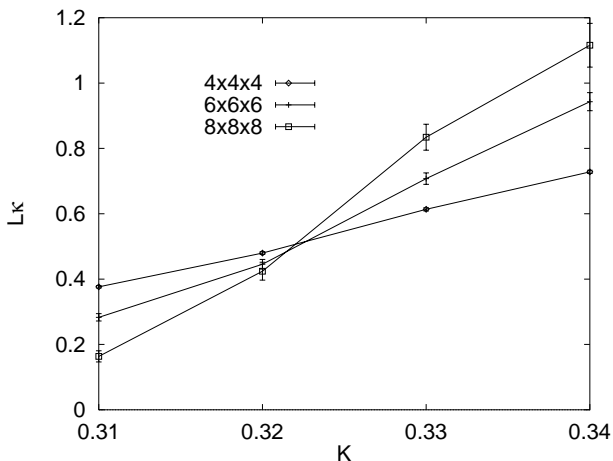

FIG. 12. The compressibilty at the tip of the lobe ($\Delta = 0.2, \mu = 1.0$) for different sytem sizes. The aspect ratio is constant for $z = 1$. The intersection point coincides with the one for the stiffness in Fig. 10 within the error bars.

Considering the above results for the stiffness and the compressibility, we conclude that below $K_C = 0.325$ we have indeed a Mott insulating phase and for $K > K_C$ a

superconducting phase, in particular there is no sign of an intervening Bose glass phase.
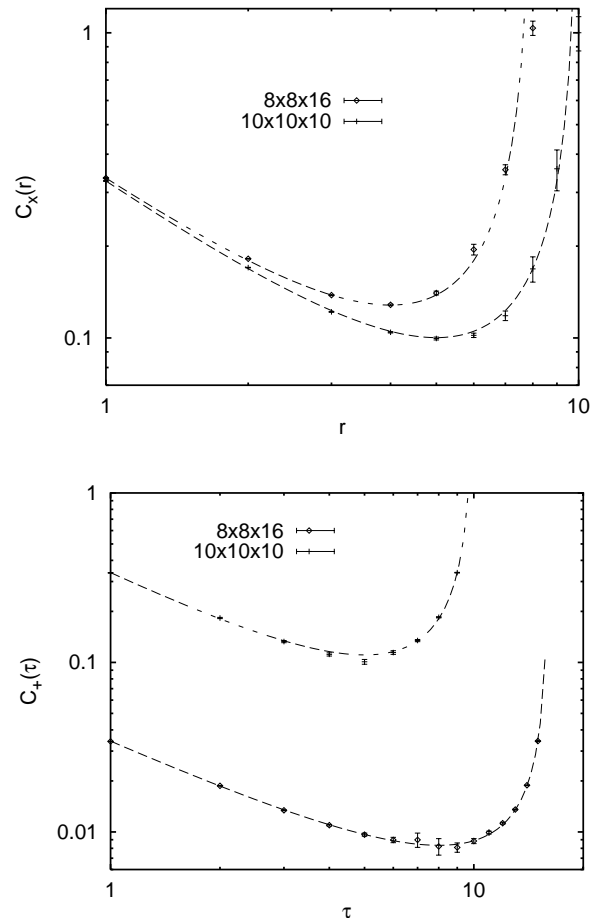

FIG. 13. The correlation functions $C_x(r)$ (top) and $C_+(\tau)$ (bottom) for system sizes 8x8x16 and 10x10x10 at the critical point $K_C = 0.325$. The dashed lines are fits to $C_x(r) = a(r^{y_x} + (L - r)^{y_x})$ and $C_+(\tau) = b(\tau^{y_\tau} + (L_\tau - \tau)^{y_\tau})$ respectively. We obtain $z = y_x/y_\tau = 1$ independent of the shape of the sample.

We can now go for the consistency check of our assumed value of $z = 1$. Therefore we measure the spatial- and imaginary time correlation functions as given by eq. (20) and (22). From these functions we obtain the exponents y_x and y_τ and then z is simply given by eq. (27), i.e. $z = y_x/y_\tau$. Fig. 13 shows the correlation functions for different system sizes at criticality $K_C = 0.325$. By fitting to the functions $C_+(\tau) = a(\tau^{-y_\tau} + (L_\tau - \tau)^{-y_\tau})$ and $C_x(r) = a'(r^{-y_x} + (L - r)^{-y_x})$ respectively we obtain $y_\tau = 1.11 \pm 0.02$, $y_x = 1.07 \pm 0.02$ for system size 10x10x10 and $y_\tau = 1.10 \pm 0.02$, $y_x = 1.10 \pm 0.02$ for system size 8x8x16. This yields $z = y_x/y_\tau = 1$ in both cases, confirming the value used in the scaling analysis of the stiffness and the compressibility and demonstrating that z is indeed independent of the shape of the sample. Additionally from y_x and y_τ the critical exponent η can be obtained according to eq. (28), which yields

$\eta = 0.1 \pm 0.1$.

To summarize the above scaling analysis, we find a direct Mott insulator to superconductor transition with no intervening Bose glass phase at the multicritical point $\mu = 1$. The critical exponents are $z = 1$, $\nu = 0.7 \pm 0.1$ and $\eta = 0.1 \pm 0.1$. These are very close to the exponents obtained for the 3D XY-model both analytically from ϵ-expansions[26] $\nu = 0.669 \pm 0.002$, $\eta = 0.033 \pm 0.004$ and by Monte Carlo simulations[7] where $\nu = 0.667$ and $\eta \approx 0.02$ were obtained. Thus we conclude that the universality class of the transition is not changed by weak disorder. However, this might be different for stronger disorder, and for instance for $\Delta = 0.4$ we get an effective exponent $z = 1.4$.

Furthermore we want to comment on the result $\nu = 0.7$. This value of ν seems to contradict the inequality $\nu \geq 2/d$[27,28], where d is the dimension in which the system is disordered (i.e. here $d = 2$), which should be applicable to a broad class of phase transitions that can be triggered by the strength of the disorder. However, by comparing the critical couplings for the MI-SF transition for the pure case $K_C(\Delta = 0, \mu = 1) = 0.333 \pm 0.003$ and weak disorder $K_C(\Delta = 0.2, \mu = 1) = 0.325 \pm 0.002$ it becomes evident, that the position of the tip of the lobe only depends very weakly on the disorder strength or is even independent of it, at least for small disorder. Thus this transition cannot be triggered by varying the disorder strength and therefore the inequality possibly does not apply here. We also want to mention the possibility, that our data are not yet in the asymptotic scaling regime and therefore the measured exponent ν is only an effective exponent for small length scales, although we find this very unlikely due to the quality of the scaling plots.

We remark that we also find an intersection point in the finite size scaling plot of the stiffness at $K = 0.32$ (which is close to the critical coupling $K_C = 0.325$ we find for $z = 1$) when assuming $z = 2$, even though this intersection point is not as convincing as the one for $z = 1$. However, as pointed out above, by calculating the correlation functions we always obtain $z = 1$, independent of the shape of the sample. Furthermore there is no intersection point in the plot of the compressibility for $z = 2$. Thus a transition with $z = 2$, which could indicate a transition from the Bose glass phase, is ruled out by the above results.

B. The Mott Insulator - Bose glass transition

As we have seen the BG phase is quite similar to the quantum Griffith phase occuring in random transverse Ising models. One can extend the analogy to the other phases, too, and formulate the following dictionary (see Table I):

One can identify the Mott insulating and paramagnetic phases as the disordered phases, the Bose glass and the Griffiths phase as the weakly or locally ordered phases and the superfluid and ferromagnetic phase as the ordered phases. The transition from the insulating BG phase to the superconducting phase as well as the transition from the paramagnetic Griffiths phase to the ferromagnetic phase are both second order, whereas the MI-BG and PM-Griffiths "transitions" are in fact *not* real phase transitions: only some susceptibility starts to diverge due to local effects, which for the Bose glass phase also implies that it becomes compressible. As in the context of the Griffiths phase, where a continuously increasing (coming from the disordered phase) dynamical exponent leads to this divergence, no diverging length scale is connected with the closing of the gap upon entering the Bose glass phase (coming from the Mott insulator).
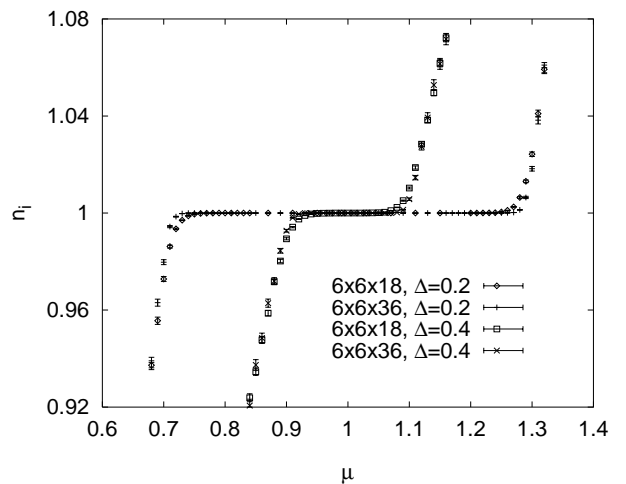

FIG. 14. Number of particles per site vs. chemical potential at $K = 0.19$ for different system sizes and different disorder strengths Δ. In the Mott phase the particle number is fixed at an integer value. For increasing disorder ($\Delta = 0.4$) the Mott phase shrinks.

As a consequence we cannot locate the MI-BG transition via finite size scaling. To get an idea of the phase diagram, we measure the particle number n_i per site as a function of the chemical potential μ at fixed coupling $K = 0.19$. This corresponds to moving along the line through point #2 in Fig. 1. We choose the value of $K = 0.19$ as to be below the critical coupling $K_C(\Delta = 0.2, \mu = 0.5) = 0.20$ for the BG-SF transition (Point #3 in Fig. 1). Such a plot is shown in Fig. 14 for $K = 0.19$. The different curves correspond to different system sizes. One observes that starting at the chemical potential $\mu = 0.65$ the particle number per site increases with roughly constant slope. This means, that the compressibility $\kappa = \partial n / \partial \mu$ is indeed finite in a certain range of the chemical potential. For $\mu \approx 0.73$ the particle number per site reaches one, meaning that we are in the Mott insulating phase. Increasing the chemical potential further does not change the number of particles, which means that the compressibility vanishes as

12

expected. For higher values of μ, we leave the Mott phase and again have a phase with non vanishing compressibility. For stronger disorder ($\Delta = 0.4$) one observes a similar behaviour, but the range of the chemical potential where the particle number is constant is smaller. This indicates that with increasing disorder the Mott lobes indeed shrink, as the disorder reduces the energy gap in the MI phase.

In Fig. 15 we show the number of particles vs. chemical potential near the tip of the lobe. It can be seen that at the critical point $K_C(\Delta = 0.2, \mu = 1) = 0.325$ there is no longer a range of the chemical potential where the number of particles is constant demonstrating that the MI phase disappears at K_C.
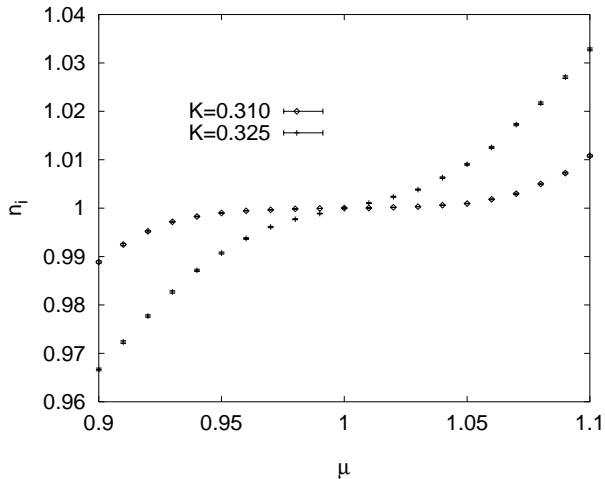

FIG. 15. Number of particles per site vs. chemical potential for $\Delta = 0.2$ near the tip of the lobe for system size 6x6x18, demonstrating that the Mott lobe disappears at $K_C = 0.325$.
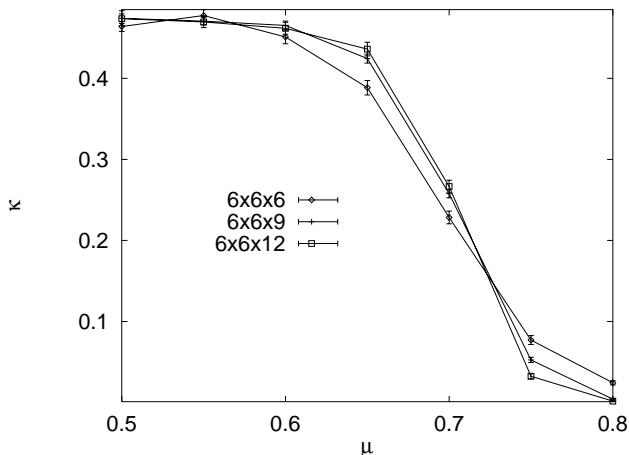

FIG. 16. The compressibility κ as a function of the chemical potential μ for the Mott insulator to Bose glass transition at fixed $K = 0.19$ ($\Delta = 0.2$).

We also calculate the compressibility directly as function of μ at the same value of $K = 0.19$ as above, which is shown in Fig. 16. As long as the typical length scale ξ

at the MI-BG transition (which does *not* diverge here, as we mentioned above) is smaller than the system size L, the compressibility κ will not depend significantly on L. Indeed we observe a much stronger dependence on L_tau, which is due to the closing of the gap at the MI-BG transition. In Fig. 16 we demonstrate this effect by showing data for increasing system size in the imaginary time direction and constant system size in the space direction. The curves intersect at $\mu = 0.73$, which corresponds to the left edge of the MI-plateau in Fig. 14, i.e. the MI-BG transition point. For increasing L_τ the curves become steeper and one might guess that in the limit $L_\tau \to \infty$ the compressibility jumps discontinuously from $\kappa = 0$ for $\mu > 0.73$ (in the MI-phase) to a finite value ($\kappa \approx 0.5$) for $\mu < 0.73$ (in the BG phase). Unfortunately the sample to sample fluctuations of κ are extremely large so that we could not get good enough statistics for larger values of L_τ.

A discontinuity in the compressibility would support the conjecture that the MI-BG transition is first-order[5]. At a generic first order phase transition one expects a phase coexistence, which in our case means the coexistence of the compressible BG and the incompressible MI phase at $\mu \approx 0.73$. Such a possibility can be studied systematically[25] via the calculation of the probability distribution $P(\kappa)$ of the compressibility in finite systems. If the MI-BG transition is first order and shows phase coexistence, one expects a double peak structure in $P(\kappa)$ with a peak at zero (from MI phase) and at ≈ 0.5 (from the BG phase). However, our data for $P(\kappa)$ (see Fig. 17) show only a single peak moving from $\kappa = 0$ to $\kappa \sim 0.5$ when increasing μ from below to above the transition, which excludes phase coexistence.
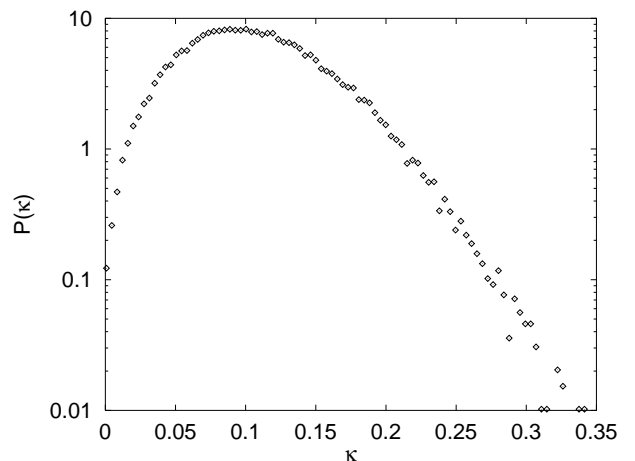

FIG. 17. The probability distribution $P(\kappa)$ of the compressibility for system size 6x6x9 at $\mu = 0.73$ and $K = 0.19$ ($\Delta = 0.2$). Note the logarithmic scale of the y-axis and the exponential tail of the distribution.

C. The local susceptibility in the Mott insulating and superfluid phase

Finally we consider the probability distribution $P(\ln \chi)$ of the local susceptibility in the Mott insulating and the superfluid phase. We fix the chemical potential at $\mu = 1$, i.e. we are at the tip of the lobe and calculate $P(\ln \chi)$ for different couplings K. The resulting curves are shown in Fig. 18. From the preceding section we know that the Mott insulator to superfluid transition for $\Delta = 0.2$ and $\mu = 1.0$ is at $K_C = 0.325$. For the smallest value of $K = 0.250$, which clearly is in the Mott insulating phase, one observes that $P(\ln \chi)$ has no tail as in the Bose glass phase but rather abruptly decays to a very small value. This indicates that in the MI phase one has indeed a finite energy gap. At criticality, i.e. at $K = 0.325$, the imaginary time Green's function decays algebraically with an exponent close to one (≈ 1.1, see Fig. 13). Since $\int d\tau C(\tau) \sim \int d\chi \chi P(\chi)$, we again expect a probability distribution $P(\ln \chi)$ with a $1/\chi$ tail, which is verified by comparison with the dashed line in Fig. 18. For higher values of K in the superfluid phase the curves are shifted to the right, and one again has an algebraic tail.
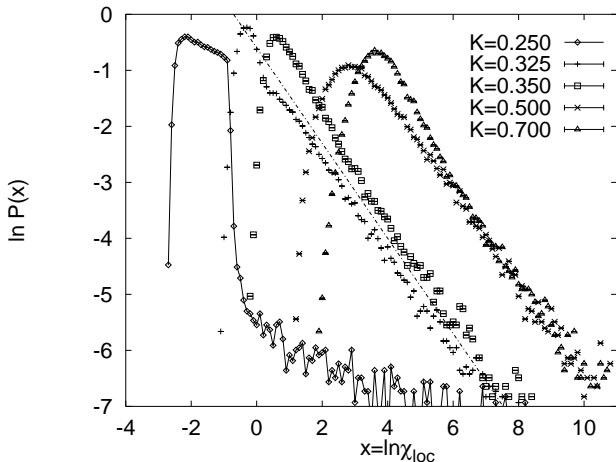

FIG. 18. The probability distribution $P(\ln \chi_{loc})$ of the local susceptibility in the Mott insulating and the superfluid phase as a function of K for $\Delta = 0.2$ and $\mu = 1$. The MI-SF transition is at $K_C = 0.325$. In the MI phase ($K = 0.250$) the distribution $P(\ln \chi)$ has no tail, indicating a finite energy gap. At criticality and in the SF phase one recovers a tail. The dashed line has slope -0.9.

VII. SUMMARY AND DISCUSSION

Concluding we have shown that the Bose glass phase shares many features with the Griffiths phase in random transverse field Ising systems. We find an algebraic decay of the imaginary time Green's function, a broad probability distribution of the local susceptibility with an $1/\chi^2$ tail and thus a diverging global superfluid susceptibility.

The occuring singularities can be parametrized by a dynamical exponent $z = 2$ which is constant in the Bose glass phase. This dynamical exponent z is equal to the critical dynamical exponent $z = d = 2$ for the Bose glass superfluid transition and it is an open question whether this equality holds in general, since the exponents have their origin in different physics. We remark that this equality was also found to hold in the random transverse Ising chain[12] and in the random transverse Ising spin glass[13].

By calculating the participation ratio we were able to show that the excitations in the Bose glass phase are fully localized. This is in contrast to the random transverse Ising systems, since in these models rare strongly coupled *clusters* of spins act collectively giving rise to a divergent susceptibility. Furthermore we find the participation to obey a scaling relation.

The investigation of the phase transition at the tip of the lobe for integer boson densities showed a *direct* Mott insulator to superconductor transition for weak disorder. The critical exponents we obtain are $z = 1, \nu = 0.7 \pm 0.1$ and $\eta = 0.1 \pm 0.1$ which agree with the exponents of the pure 3D XY model, so the universality class of the transition is not altered by weak disorder. This conclusion is supported by recent mean field renormalization group studies and scaling arguments put forward in[29].

VIII. ACKNOWLEDGEMENTS

d. B-H-M			RTIC		
Mott insulator	χ_{loc}	finite	Paramagnetic phase	χ_{loc}	finite
	ρ	$= 0$		m	$= 0$
Bose glass	χ_{loc}	div.	Griffiths phase	χ_{loc}	div.
	ρ	$= 0$		m	$= 0$
superfluid/	χ_{loc}	div.	Ferromagnetic phase	χ_{loc}	div.
superconducting	ρ	$\neq 0$		m	$\neq 0$
	"ordered"			"ordered"	

TABLE I. Corresponding phases in the disordered boson Hubbard model (d. B-H-M) and the random transverse Ising chain (RTIC). ρ is the superfluid stiffness, m the spontaneous magnetization and χ_{loc} the local susceptibility.

[1] Y. Liu et al. Phys. Rev. Lett. **67**, 2068(1991); M. A. Palaanen, A. F. Hebard and R. R. Ruel, Phys. Rev. Lett. **69**, 1604 (1992).

[2] P. A. Crowell, F. W. Van Keuls and J. D. Reppy, Phys. Rev. Lett. **75**, 1106 (1995); P. A. Crowell et al, Phys. Rev. B **51**, 12721 (1995).

[3] M. P. A. Fisher, P. B. Weichman, G. Grinstein, D. S. Fisher, Phys. Rev. B. **40**, 546 (1988).

[4] K. G. Singh and D. Rokshar, Phys. Rev. B **46**, 3002(1992).

[5] J. K. Freericks and H. Monien, Phys. Rev. B **53** (1996).

[6] R. T. Scalettar, G. G. Batrouni, G. T. Zimanyi, Phys. Rev. Lett. **66**, 3144 (1991) and G. G. Batrouni and R. T. Scalettar, Phys. Rev. B **46**, 9051 (1991).

[7] E. S. Sørensen, M. Wallin, S. M. Girvin and A. P. Young, Phys. Rev. Lett. **69**, 828(1992); M. Wallin, E. S. Sørensen, S. M. Girvin and A. P. Young, Phys. Rev. B **49**, 12115 (1994).

[8] W. Krauth, N. Trivedi, D. Ceperly, Phys. Rev. Lett. **67**, 2307(1991).

[9] A. v. Otterlo, K. H. Wagenblast, R. Baltin, C. Bruder, R. Fazio, and G. Schön, Phys. Rev. B **52**, 16176 (1995).

[10] R. B. Griffiths, Phys. Rev. Lett. **23**, 17 (1969); B. McCoy, Phys. Rev. Lett. **23**, 383 (1969).

[11] D. S. Fisher, Phys. Rev. Lett. **69**, 534 (1992); Phys. Rev. B **51**, 6411 (1995).

[12] A. P. Young and H. Rieger, Phys. Rev. B **53**, 8486 (1996).

[13] H. Rieger and A. P. Young, Phys. Rev. B **54**, 3329 (1996).

[14] M. Guo, R. N. Bhatt and D. A. Huse, Phys. Rev. B **54**, 3323 (1996).

[15] J. Kisker and H. Rieger, Phys. Rev. B (RC), in press.

[16] M. P. A. Fisher, G. Grinstein, Phys. Rev. Lett. **60**, 208 (1988).

[17] M. Suzuki, Progr. Theor. Phys. **56**, 1454 (1976).

[18] J. Villain, J. Phys. **36**, 581(1975).

[19] M. P. A. Fisher and D. H. Lee, Phys. Rev. B **39**, 2756 (1989).

[20] D. M. Ceperley, Rev. Mod. Phys. **67**, 279 (1995).

[21] R. P. Feynman, Phys. Rev. B **90**, 1116 (1953); **91**, 1291 (1953); **91**, 1301 (1953).

[22] R. N. Bhatt and A. P. Young, Phys. Rev. B **37**, 5606 (1988).

[23] A. J. Bray, Phys. Rev. Lett. **60**, 720 (1988); M. Randeira, J. P. Sethna and R. G. Palmer, Phys. Rev. Lett. **54**, 1321 (1985).

[24] F. Pazmandi, G. Zimanyi and R. Scalettar, Phys. Rev. Lett. **75** 1356 (1995).

[25] K. Binder and D. P. Landau, Phys. Rev. B **30**, 1477 (1984); M. S. S. Challa and D. P. Landau, Phys. Rev. B **34**, 1841 (1986); J. Lee and J. M. Kosterlitz, Phys. Rev. B **43**, 3265 (1991).

[26] J. C. Le Guillou, J. Zinn-Justin, Phys. Rev. B **21**, 3976 (1980).

[27] A. B. Harris, J. Phys. C **7**, 1671 (1974).

[28] J. T. Chayes, L. Chayes, D. S. Fisher and T. Spencer, Phys. Rev. Lett. **57**, 2999 (1986).

[29] F. Pazmandi, G. T. Zimanyi, unpublished.

15